Volume 62
Number 13
17 February 2026
Pages 3927–4148

ChemComm

Chemical Communications

rsc.li/chemcomm

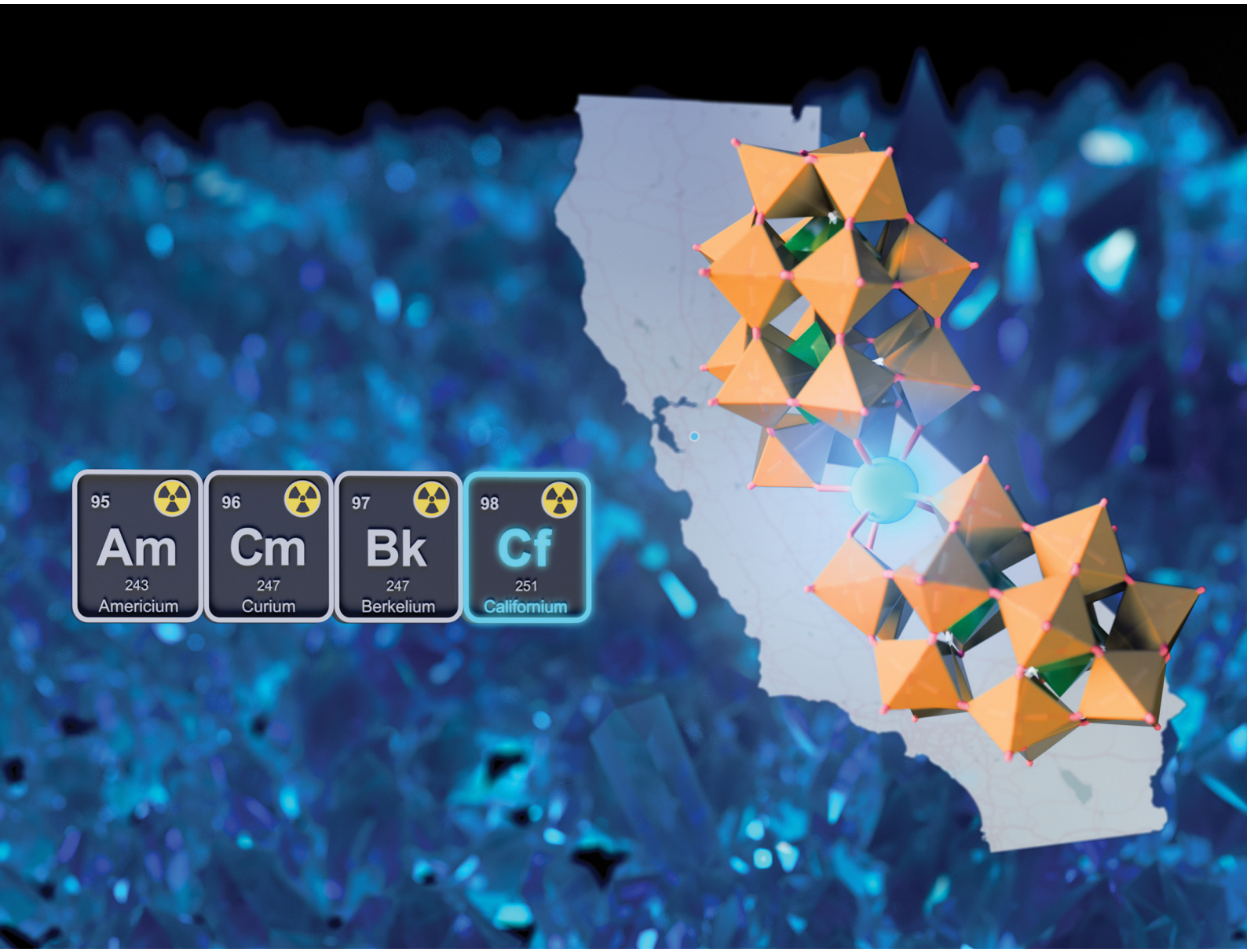

ISSN 1359-7345

ROYAL SOCIETY OF CHEMISTRY

BACK-TO-BACK COMMUNICATION ARTICLES

Ian Colliard and Gauthier J.-P. Deblonde
Actinide complexes with Wells–Dawson polyoxometalates (part 1): americium and curium
Actinide complexes with Wells–Dawson polyoxometalates (part 2): californium

ChemComm

COMMUNICATION

View Article Online
View Journal | View Issue

Cite this: *Chem. Commun.*, 2026, **62**, 4018

Received 9th December 2025,
Accepted 14th January 2026

DOI: 10.1039/d5cc06999h

rsc.li/chemcomm

Actinide complexes with Wells–Dawson polyoxometalates (part 1): americium and curium

Ian Colliard * and Gauthier J.-P. Deblonde *

We report the first trivalent actinide complexes with a Wells–Dawson polyoxometalate. Americium(III) forms two distinct phases: triclinic $K_{17}Am(P_2W_{17}O_{61})_2{\cdot}42.5H_2O$ and monoclinic $K_{17}Am(P_2W_{17}O_{61})_2{\cdot}12H_2O$. Curium(III) crystallizes as monoclinic $K_{17}Cm(P_2W_{17}O_{61})_2{\cdot}8H_2O$. XRD-quality single crystals were obtained from just ~330 nanograms of actinides. This work establishes clear structure–property relationships that will guide investigations on scarce f-elements.

Polyoxometalates (POMs) continue to be powerful platforms for stabilizing and characterizing f-element complexes due to their rigid metal-oxide frameworks, high charge, and tunable lacunary binding pockets.[1–3] Within the ever-expanding family of POMs, the Wells–Dawson[4] anion α-$[P_2W_{18}O_{62}]^{6-}$ and its monolacunary derivative $[P_2W_{17}O_{61}]^{10-}$ (abbreviated P_2W_{17}) are perhaps the most widely studied,[5] on par with the Keggin[6] POMs and Weakley-Peacock[7] POMs. The P_2W_{17} structure is particularly attractive because its set of four O-donor enforces a highly symmetric and reproducible coordination environment around the cations it complexes. This water-soluble ligand has enabled extensive systematic studies across the lanthanide series to characterize its "sandwich complexes", $[Ln^{III}(P_2W_{17})_2]^{17-}$, both in solution and in the solid-state.[8–15] These studies included ^{31}P and ^{183}W NMR characterization, luminescence studies, EXAFS studies, and more. The first single crystal structure of a $[Ln^{III}(P_2W_{17})_2]^{17-}$ complex was reported in 2001 by Luo *et al.*:[10] $K_5Na_6(H_3O)_6[La(P_2W_{17}O_{61})_2]{\cdot}49H_2O$ (Table S1). Since then several $[Ln^{III}(P_2W_{17})_2]^{17-}$ and also $[Ln^{IV}(P_2W_{17})_2]^{16-}$ crystal structures have been reported, including a complete series with the more specialized derivatives $[Ln^{III}(P_2W_{17})_2(proline)]^{17-}$ (Ln = La to Lu, except Pm) reported by Iijima *et al.* in 2018.[8,12,13]

In contrast, the chemistry of P_2W_{17} with actinides, especially trivalent actinides, remains relatively unexplored. Pioneering studies from Francesconi, Soderholm, Antonio, and co-workers probed the speciation of tetravalent actinides (Th^{4+}, U^{4+}, Np^{4+}, Pu^{4+}) and trivalent actinides (Np^{3+}, Pu^{3+}, Am^{3+}) in the presence of P_2W_{17} *via* EXAFS and cyclic voltammetry.[9,16] In terms of solid-state structures, prior to the present study (compiled in Table S2), only P_2W_{17} complexes with tetravalent actinides had been reported. A 2003 study from Ostuni *et al.*[17] reported the first structures of Wells–Dawson complexes containing actinide ions, namely Th(IV) and U(IV) (Table 1). Then in 2009, a breakthrough study from Sokolova *et al.*,[18] determined the single crystal structures of five tetravalent actinide complexes of P_2W_{17}, namely $[An(P_2W_{17})_2]^{16-}$ with An = Th^{4+}, U^{4+}, Np^{4+}, Pu^{4+}, and Am^{4+}. Remarkably, Sokolova *et al.* established the reaction of the P_2W_{17} complex with $K_2S_2O_8$ that allows for the oxidation Am^{3+} and stabilization Am^{4+}. To this date, this remains a very rare example of tetravalent americium coordination compound. Authors from the same team had also previously reported the same kind of reactions to stabilize Tb(IV) and Pr(IV) in aqueous solution with P_2W_{17}.[19,20] The formation of stable complexes between tetravalent cations and P_2W_{17} was well-established which ultimately led to the isolation of the tetravalent actinides series (Th, U, Np, Pu, and Am) reported in 2009 (Table S2).

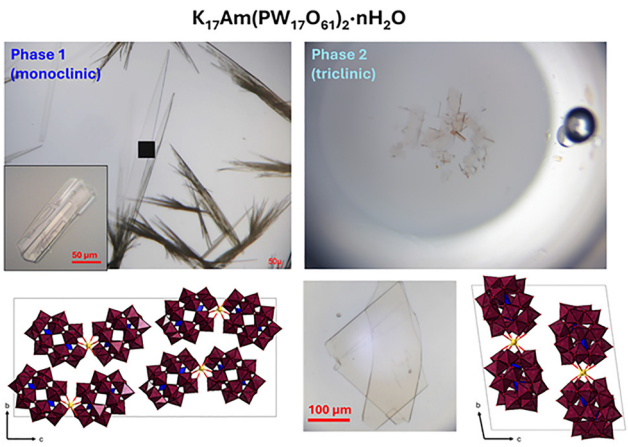

Fig. 1 Pictures of the two different phases of $[Am^{III}(P_2W_{17})_2]^{17-}$ isolated in this study. Unit cells are viewed along the *a*-axis. W in maroon, P in blue, O in red and Am in gold.

Lawrence Livermore National Laboratory, Livermore, California 94550, USA. E-mail: Colliard1@LLNL.gov, Deblonde1@LLNL.gov

Table 1 Structural parameters for the Am(IV) *versus* Am(III) and Cm(III) Wells–Dawson complexes. See Table S1 for relevant analogous lanthanide(III) compounds previously reported and new structures for $Pr^{III}(P_2W_{17})_2$ and $Nd^{III}(P_2W_{17})_2$ obtained in the present study. See Tables S3 and S4 for more details

Compound	$Am^{IV}(P_2W_{17})_2$	$Am^{III}(P_2W_{17})_2$	$Am^{III}(P_2W_{17})_2$	$Cm^{III}(P_2W_{17})_2$
Structure type	Triclinic $P\bar{1}$	Triclinic $P\bar{1}$	Monoclinic $P2_1/n$	Monoclinic $P2_1/n$
⟨Am–O⟩	2.325 Å	2.433(5) Å	2.450(27) Å	2.44(7) Å
P1–Am–P1′ bent	161.9°	160.0°	169.1°	169.9°
P2–Am–P2′ bent	130.4°	128.5°	138.5°	138.2°
Ref.	18	This work	This work	This work

However, despite the large number of studies on Wells–Dawson complexes, no complex containing an An(III) ion and a Wells–Dawson ligand has been isolated to date. This apparent gap is notable as the 5f electronic structure of An(III) ions may produce distinct binding preferences, structural distortions, or even new phases relative to their Ln(III) or An(IV) analogues. Recent advances in microscale and nanoscale syntheses have now made such studies feasible. Our group previously demonstrated that lacunary POM ligands can unlock crystallographic characterization of actinides from as little as ~2 to 10 μg of the radioisotope.[21–28] Here, we further expand this strategy, with an optimized crystallization approach that reliably produces XRD-quality single crystals from sub-microgram quantities of Am^{3+} and Cm^{3+}. This enhancement permits direct structural comparison between lanthanide(III/IV) and actinide(III/IV) complexes of P_2W_{17}. In this work, we report the first known trivalent actinide Wells–Dawson complexes: two phases of Am^{3+} (triclinic and monoclinic) and one phase of Cm^{3+} (monoclinic). We also isolated previously missing structures with Pr^{3+} and Nd^{3+}. We analyze the structural distortions, bending, twisting, and metal–oxygen distances, that differentiate these phases and correlate them with changes observed in solution and solid-state UV-vis-NIR spectroscopy. The combined structural and spectroscopic data establish clear phase-dependent structure–property relationships and position lacunary Wells–Dawson POMs as versatile scaffolds for exploring the coordination chemistry of f-elements, including the rarest ones.

Upon formation of the $[Am^{III}(P_2W_{17})_2]^{17-}$ complex (abbreviated $Am^{III}(P_2W_{17})_2$) in aqueous solution, it can be precipitated and crystallized by introduction of K^+ counterions in the system. This Am(III)-POM compound appears orange (Fig. 1) and two distinct phases were clearly visible in the samples, depending on the excess of KCl added. The scXRD analysis revealed two distinct structures: a triclinic phase fully formulated as $K_{17}Am(P_2W_{17}O_{61})_2{\cdot}42.5H_2O$ in the space group $P\bar{1}$, with a unit cell volume of 7850.7 $Å^3$. The other phase is monoclinic and is fully formulated as $K_{17}Am(P_2W_{17}O_{61})_2{\cdot}12H_2O$, with the $P2_1/n$ space group and a unit cell volume of 15064.0 $Å^3$. Using the same synthetic route with curium, we only obtained one type of crystals, which looked colorless and with a morphology similar to the monoclinic phase obtained with americium. Single crystal XRD analysis confirmed that, under our experimental conditions, curium only leads to the monoclinic phase, which is fully formulated $K_{17}Cm(P_2W_{17}O_{61})_2{\cdot}8H_2O$, in the $P2_1/n$ space group, and with a unit cell volume of 15064.0 $Å^3$.

Focusing on the Am(III) structures, the truly different unit cells of the two phases rationalize their visually distinct crystal morphologies (*i.e.*, needle-like *versus* flat – Fig. 1). However, while both phases feature the same $Am^{III}(P_2W_{17})_2$ complex, there are key structural differences that manifest themselves in the crystal structures and in the spectroscopic characterization. We previously proposed a framework of structural metrics to describe actinide and lanthanide complexes with another type of POMs, *i.e.*, the Keggin complexes $[M(XW_{11}O_{39})_2]^{n-}$ (X = B^{3+}, Si^{4+}, P^{5+}, Ge^{4+}, Ga^{3+}).[22–26] These metrics apply to the Wells–Dawson complexes too. Notable differences between the two $Am^{III}(P_2W_{17})_2$ structures are the Am–O bond lengths (Fig. S3), bending and twisting of the overall complex (Table 1), and the counterions positions (Fig. S4). The two morphologies seen for $Am^{III}(P_2W_{17})_2$ can be crystallographically described by one asymmetric unit, meaning there is only one unique species describing each structure. When comparing each unit cell, the principal symmetry axis for $Am^{III}(P_2W_{17})_2$ generally lies parallel to the *c*-axis. This makes the *c*-axis sensitive to Am–O bond lengths, and the *a*- and *b*-axis are sensitive to twisting of the whole complex (Fig. 1). As such, when one compares each axis length, with the *c*-axis for the monoclinic phase divided by two, there is no exact match. Indicating that while the triclinic and monoclinic phase contain the same complex, each induces slight differences to the complex and around Am(III). Across the structures reported here, the monoclinic phase displays more relaxed coordination metrics: smaller bending angles (P1–Am–P1′ = 169.1°; P2–Am–P2′ = 138.5°), a significantly reduced twisting of the two P_2W_{17} units (2.00°), and the 17 K^+ counterions further away from the Am(III) complex (Fig. S4). In contrast, the triclinic phase exhibits higher bending angles (160.0° and 128.5°, respectively) alongside a pronounced twist (8.88°). These differences correspond to a more strained environment in the triclinic structure.

Curium(III), meanwhile, crystallizes exclusively in the monoclinic phase, with bending and twisting metrics nearly identical to those of the $Am^{III}(P_2W_{17})_2$ monoclinic form. The average Cm–O bond distance (2.44(7) Å) is consistent with its slightly smaller ionic radius[21,29,30] relative to Am(III) and follows the smooth contraction trend established across the f-element series (Fig. 4). These complexes exhibit polymorphism with only minor distortion reflecting the intrinsic changes from the packing environment of these complexes. The close structural match between $Am^{III}(P_2W_{17})_2$ and $Cm(P_2W_{17})_2$ in the same phase further emphasizes the importance of phase-matching when comparing structural metrics across f-element complexes. Raman analysis (Fig. S1) revealed that there is little difference between the two $Am^{III}(P_2W_{17})_2$ phases. Therefore, we

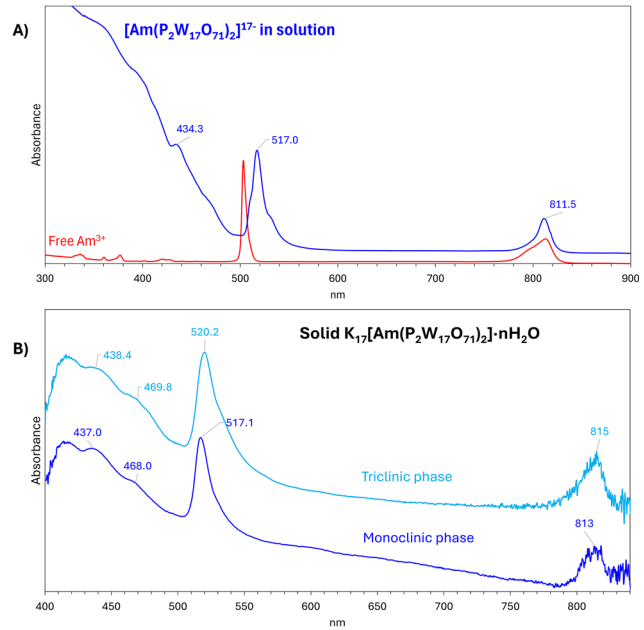

Fig. 2 Absorbance of Am^{3+} complexed to the Wells–Dawson POM ligand $P_2W_{17}O_{61}^{10-}$. (A) Solution-state UV-vis-NIR absorbance spectrum of $[Am^{III}(P_2W_{17})_2]^{17-}$ in aqueous solution. The spectrum of uncomplexed Am^{3+} in 0.1 M HCl is also given for comparison. (B) Solid-state UV-vis absorbance spectrum of the two phases of $K_{17}Am(P_2W_{17}O_{61})_2{\cdot}nH_2O$ (monoclinic and triclinic phases – see Table 1 and text). The absorbance spectrum for the equivalent complex with curium, $[Cm^{III}(P_2W_{17})_2]^{17-}$, is given in Fig. S2.

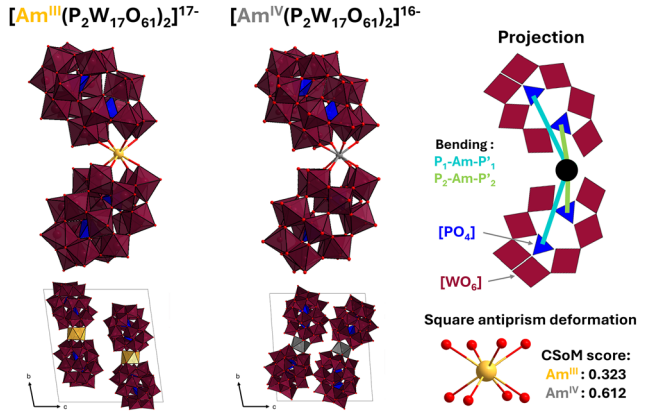

Fig. 3 Comparison of the $Am^{IV}(P2W17)_2$ structure (Sokolova *et al.*[18]) and the equivalent $Am^{III}(P2W17)_2$ structure obtained in the present study. On the right, the projection of the complex' geometry shows bending angles and the potential twisting of the structure. The symmetry of both AmO_8 octahedra was quantified using Continuous Symmetry operation Measure (CSoM), as defined by Nielsen & Sørensen (see Table S5).[31]

can conclude that the observed structural differences have little effect on the vibrational nodes for these complexes.

However, we noted measurable differences in the electronic absorbance of the two structures. The solution UV-vis-NIR absorbance spectrum of $Am^{III}(P_2W_{17})_2$ shows complete complexation with the main 5f–5f band of Am^{3+} shifting from 503.0 nm to 517.0 nm (Fig. 2A). In solid-state, the two phases of the $Am^{III}(P_2W_{17})_2$ exhibit noticeable differences, with the main absorbance band for the monoclinic phase centered at 517.1 nm, while the same band shifts to 520.2 nm for the triclinic phase. Slight differences are also observed for the other characteristic bands of Am^{3+} (Fig. 2B). Aside from hydration numbers, the main structural differences between the monoclinic and triclinic phases for $Am^{III}(P_2W_{17})_2$ are Am–O bond lengths (Fig. S3), the bending and twisting (Table 1), and the Am–K distances (Fig. S4).

As described above, the triclinic phase is more strained by the higher bending and twisting of the P_2W_{17} unit. The monoclinic phase, which had thus far remained elusive (Table S1), even for the equivalent lanthanide complexes, exhibits a more linear complex, with smaller bent angle and less twisting (Table 1). When comparing the absorbance spectra of the two phases *versus* the aqueous absorbance, the monoclinic phase appears as an almost perfect match for the aqueous complex. As we expect the complex to be more flexible in solution (due to dynamic solvent exchange and rotation), the monoclinic phase appears as an intermediate state between the average structure of the complex in solution and the triclinic phase.

Comparisons of the similar complexes under different phases can be useful when trying to extract information on the structure variability of a given metal–ligand system. It is, however, essential that for polymorphic systems, phase matching is verified when comparing structures across different metals or different oxidation states of the same metal.

We can exemplify this by looking at the $Am^{III}(P_2W_{17})_2$ structures reported here and the equivalent triclinic Am^{IV}-$(P_2W_{17})_2$ structure previously reported by Sokolova *et al.*[18] Both share the same stoichiometry, same coordination environment, and have a related triclinic phase (Fig. 3 and Table 1). The most noticeable difference from $Am^{IV}(P_2W_{17})_2$ to $Am^{III}(P_2W_{17})_2$ is the shortening of the Am–O bond lengths, 2.325 Å from 2.433(5) Å. However, while there is a contraction of Am–O bond lengths, counterintuitively, both bending angles (P1–Am–P1 and P2–Am–P2, see Table 1 and Table S3) relax by almost 2° when going from the Am(III) to Am(IV) structure. However, while $Am^{IV}(P_2W_{17})_2$ is less bent, the structure accommodates the shorter Am–O distances by twisting more, by about 2.7°. It is important to note that the comparison of the $Am^{IV}(P_2W_{17})_2$ structure (*i.e.*, triclinic) with the non-isomorphic structure of $Am^{III}(P_2W_{17})_2$ (*i.e.*, the monoclinic one) would result in the ascription of higher degrees of structural shifts that may not necessarily originate from the oxidation Am^{3+}-to-Am^{4+}. It is therefore imperative that extrapolation of f-element properties across POM complexes be done in a consistent manner, with truly comparable structural datasets. This statement is further supported by extending structural comparisons to lanthanides.

Our expanded dataset reveals previously unrecognized polymorphism within the series of lanthanide(III) complexes with P_2W_{17}, with the monoclinic phase also obtained for $Pr^{III}(P_2W_{17})_2$ (Table S1). We also report the triclinic phase for $Nd^{III}(P_2W_{17})_2$ (Table S4). Although $An^{IV}(P_2W_{17})_2$ complexes were already known to crystallize in multiple phases,[18] no $Ln^{III}(P_2W_{17})_2$ complex had been observed to adopt distinct crystallographic packings while retaining identical primary coordination

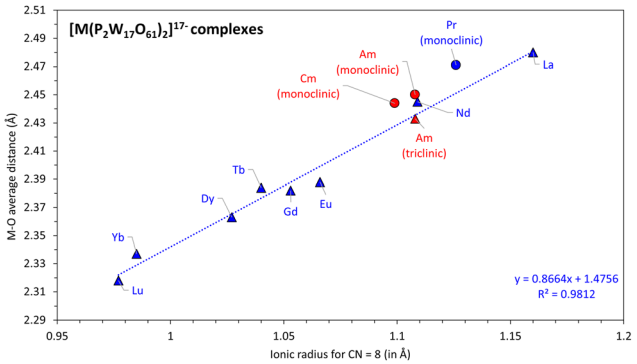

Fig. 4 Correlation between the average metal-oxygen bond distance in $[M(P_2W_{17}O_{61})_2]^{17-}$ and the ionic radius of the f-element. Triangles: Triclinic phases. Circle: Monoclinic phases. Ionic radius of the Ln(III) were taken from Shannon's list[29] (coordination number of 8). For Am^{3+}, see Cross *et al.* 2012.[32] For Cm^{3+}, see Colliard *et al.* 2022.[21]

environments. Since $Ln^{III}(P_2W_{17})_2$ complexes can crystallize in both triclinic and monoclinic forms, phase matching accordingly becomes ever more important. Looking at just the Ln(III)–O and An(III)–O bond lengths (Fig. 4), distinct trendlines emerge for the triclinic and monoclinic phases. For these Ln systems, the M–O bond lengths, bending metrics, and twisting distortions differ subtly, but systematically, between phases, leading to parallel but offset structural trendlines. Average Ln–O bond distances within the triclinic phase are consistently shorter and accompanied by greater ligand distortion, mirroring the strained environment observed for the Am(III) triclinic structure (Fig. 4). Conversely, the monoclinic Ln(III) phases display more relaxed bending and minimal twisting, yielding bond lengths that fall on a distinct and internally consistent trend. This polymorphism demonstrates that comparisons of metal–oxygen bond distances across the lanthanide and actinide series cannot be made without strict phase matching: mixing triclinic and monoclinic structures artificially broadens the apparent crystallographic ionic radius trend and obscures true electronic effects. The lanthanide polymorphs thus provide a structural analogue to the Am(III) and Am(IV) case above, reinforcing that accurate cross-element comparisons rely on isolating phase-specific contributions from redox-induced or f-electron–driven changes.

Our efforts over the past few years led to the isolation of several actinide-POM and lanthanide-POM complexes from microscale syntheses.[21–24,26,28,33] While the Wells–Dawson POM was part of our initial milestone study on the subject,[21] we had not reported its actinide(III) compounds yet. Further optimization of our microscale approach to the sub-microgram realm yielded XRD quality crystals of $Am^{III}(P_2W_{17})_2$ and $Cm^{III}(P_2W_{17})_2$ with as low as ~330 ng. The emergence of two different phases for Am(III), and one for Cm(III) reveals that P_2W_{17} supports multiple coordination regimes distinguishable by characteristic morphologies, bending and twisting distortions. These geometric differences directly modulate the ligand field, producing measurable, phase-dependent changes in the electronic absorption spectra. In line with our prior studies, the ability to crystallize and characterize such complexes from nanogram quantities of isotopes opens new possibilities for the structural chemistry of scarce f-elements, including those other than americium and curium.

This material is based upon work supported by the U.S. Department of Energy, Office of Science, Office of Basic Energy Sciences, Heavy Element Chemistry program at Lawrence Livermore National Laboratory under Contract DE-AC52-07NA27344. Release number: LLNL-JRNL-2014221.

Conflicts of interest

There are no conflicts to declare.

Data availability

The data supporting this article has been included as part of the supplementary information (SI). Supplementary information is available. See DOI: https://doi.org/10.1039/d5cc06999h.

CCDC 2512143–2512147 contain the supplementary crystallographic data for this paper.[34a–e]

References

1 M. Nyman, *Dalton Trans.*, 2011, **40**, 8049–8058.
2 T. Auvray and E. M. Matson, *Dalton Trans.*, 2020, **49**, 13917–13927.
3 N. I. Gumerova and A. Rompel, *Chem. Soc. Rev.*, 2020, **49**, 7568–7601.
4 B. Dawson, *Acta Crystallogr.*, 1953, **6**, 113–126.
5 D. Nowicka, N. Vadra, E. Wieczorek-Szweda, V. Patroniak and A. Gorczyński, *Coord. Chem. Rev.*, 2024, **519**, 216091.
6 J. F. Keggin, *Proc. R. Soc. London, Ser. A*, 1934, **144**, 75–100.
7 R. D. Peacock and T. J. R. Weakley, *J. Chem. Soc. A*, 1971, 1836–1839.
8 J. Iijima, H. Naruke and T. Sanji, *Inorg. Chem.*, 2018, **57**, 13351–13363.
9 M.-H. Chiang, L. Soderholm and M. R. Antonio, *Eur. J. Inorg. Chem.*, 2003, 2929–2936.
10 Q.-H. Luo, R. C. Howell, M. Dankova, J. Bartis, C. W. Williams, W. D. Horrocks, Y. G. Young, A. L. Rheingold, L. C. Francesconi and M. R. Antonio, *Inorg. Chem.*, 2001, **40**, 1894–1901.
11 J. Bartis, M. Dankova, J. J. Lessmann, Q.-H. Luo, W. D. Horrocks and L. C. Francesconi, *Inorg. Chem.*, 1999, **38**, 1042–1053.
12 J. Iijima, H. Naruke and T. Sanji, *Chem. Lett.*, 2012, **41**, 295–297.
13 J. Iijima and H. Naruke, *J. Mol. Struct.*, 2013, **1040**, 33–38.
14 M. R. Antonio, L. Soderholm, C. W. Williams, N. Ullah and L. C. Francesconi, *J. Chem. Soc., Dalton Trans.*, 1999, 3825–3830.
15 M. R. Antonio, J. Jing, B. P. Burton-Pye and L. C. Francesconi, *Dalton Trans.*, 2010, **39**, 7980–7992.
16 M.-H. Chiang, C. W. Williams, L. Soderholm and M. R. Antonio, *Eur. J. Inorg. Chem.*, 2003, 2663–2669.
17 A. Ostuni, R. E. Bachman and M. T. Pope, *J. Cluster Sci.*, 2003, **14**, 431–446.
18 M. N. Sokolova, A. M. Fedosseev, G. B. Andreev, N. A. Budantseva, A. B. Yusov and P. Moisy, *Inorg. Chem.*, 2009, **48**, 9185–9190.
19 V. P. Kazakov, V. V. Rykova, L. A. Khamidullina and D. D. Afonitchev, *Inorg. Chim. Acta*, 1988, **148**, 135–140.
20 A. B. Yusov, V. P. Shilov and A. M. Fedoseev, *Radiochemistry*, 2007, **49**, 135–143.
21 I. Colliard, J. R. I. Lee, C. A. Colla, H. E. Mason, A. M. Sawvel, M. Zavarin, M. Nyman and G. J.-P. Deblonde, *Nat. Chem.*, 2022, **14**, 1357–1366.
22 I. Colliard and G. J.-P. Deblonde, *JACS Au*, 2024, **4**, 2503–2513.
23 I. Colliard and G. J.-P. Deblonde, *J. Am. Chem. Soc.*, 2025, **147**, 14455–14467.
24 J. Bustos, I. Colliard, V. Stavila, D. C. Kaseman, C. A. Colla, M. Nyman and G. J.-P. Deblonde, *Inorg. Chem.*, 2025, DOI: 10.1021/acs.inorgchem.5c03627.

25 A. M. Hastings, I. Colliard, D. C. Kaseman, C. A. Colla and G. J.-P. Deblonde, *Inorg. Chem.*, 2025, **64**, 18925–18937.
26 I. Colliard and G. J.-P. Deblonde, *Chem. Commun.*, 2024, **60**, 5999–6002.
27 C. A. Colla, I. Colliard, A. M. Sawvel, M. Nyman, H. E. Mason and G. J.-P. Deblonde, *Inorg. Chem.*, 2023, **62**, 6242–6254.
28 I. Colliard and G. J.-P. Deblonde, *Inorg. Chem.*, 2024, **63**, 16293–16303.
29 R. D. Shannon, *Acta Crystallogr.*, 1976, **A32**, 751–767.
30 D. Lundberg and I. Persson, *Coord. Chem. Rev.*, 2016, **318**, 131–134.
31 V. R. M. Nielsen and T. Just Sørensen, *Nat. Commun.*, 2025, **16**, 11122.
32 J. N. Cross, E. M. Villa, S. Wang, J. Diwu, M. J. Polinski and T. E. Albrecht-Schmitt, *Inorg. Chem.*, 2012, **51**, 8419–8424.
33 I. Colliard, V. Stavila and G. J.-P. Deblonde, *Chem. Commun.*, 2025, **61**, 11858–11861.
34 (*a*) CCDC 2512143: Experimental Crystal Structure Determination, 2026, DOI: 10.5517/ccdc.csd.cc2qb2w1; (*b*) CCDC 2512144: Experimental Crystal Structure Determination, 2026, DOI: 10.5517/ccdc.csd.cc2qb2x2; (*c*) CCDC 2512145: Experimental Crystal Structure Determination, 2026, DOI: 10.5517/ccdc.csd.cc2qb2y3; (*d*) CCDC 2512146: Experimental Crystal Structure Determination, 2026, DOI: 10.5517/ccdc.csd.cc2qb2z4; (*e*) CCDC 2512147: Experimental Crystal Structure Determination, 2026, DOI: 10.5517/ccdc.csd.cc2qb306.